文章编号:1006-9941(2022)09-0886-11

Preparation of Graded Structured HMX/Al to Enhance Combustion and Pressure Output Performance

HE Qian-qian, MAO Yao-feng, WANG Jun, NIE Fu-de

(*Institute of Chemical Materials, China Academy of Engineering Physics, Mianyang* 621999, *China*)

Abstract: Aluminized explosives have been widely applied due to their high energy density and pressure output. To further enhance the secondary combustion reaction and pressure output of aluminized explosives, graded structure is designed inspired by the microstructure of bamboo. In this work, the radially-graded structured HMX/Al (RGS-HMX/Al) cylinders with three layers containing different sizes and content of Al were prepared through 3D direct writing technology. The effects of Al distribution on combustion and pressure output properties of graded HMX/Al were fully studied. For the RGS-HMX/Al cylinder with Al content of 10%, 20%, and 30% distributed from inner to outer layer, the combustion reaction and flame propagation of inner layer were faster than that of outer layer. And the pressure (2337.61 kPa) was higher than that of RGS-HMX/Al cylinder with Al content in the reverse distribution. For the RGS-HMX/Al cylinder containing Al of 10 μm, 5 μm, and 160 nm distributed from inner to outer layer, a slow combustion process with sparse bright Al droplets was observed. Moreover, the highest peak pressure (1512.65 kPa) was obtained for the RGS-HMX/Al cylinders with nAl in the middle layer, which exhibited much higher pressure output than that homogeneous HMX/Al cylinder. More importantly, bimodal pressure was observed for the RGS-HMX/Al cylinders with Al of 10 μm in the middle layer.

Key words: bio-inspired; radially-graded structure; HMX/Al composites; combustion reaction; pressure output

CLC number: TJ55 **Document code:** A **DOI:** 10.11943/CJEM2022067

0 Introduction

Aluminized explosives have been practically applied in space technology and military construction due to significantly enhanced shock waves, bubble energy, and promoted after-burning effect[1-5]. Previous studies have illustrated that the content and size of aluminum (Al) play an essential role in the secondary combustion reaction and pressure output performance of aluminized explosives[6-7]. For example, the pressure attenuation and maximal pressure of aluminized explosives can be optimized by Al content[8-10]. Meanwhile, the reduced Al size benefits to pressure output of aluminized explosives owing to the enhanced reaction kinetics[11-13]. However, a few studies have shown that Al powders with small particle size could absorb more energy in the reaction zone, which in turn reduces pressure output[1, 14]. Therefore, it is still a great challenge to strengthen energy and pressure output by tuning the content and particle size of Al powders within explosives.

The reaction process, energy and pressure output performances of energetic materials depend on the distribution of components and microstructure at the macro-scale. Constructing new structure is a versatile strategy to improve the combustion reaction and energy performances of energetic materials. MA Xiao-xia et al.[15-16] found that the "father and son" structure of energetic coordination polymers@Al

Received Date: 2022-03-29; **Revised Date:** 2022-04-29

Published Online: 2022-07-19

Project Supported: National Natural Science Foundation of China (11872341 and 22075261)

Biography: HE Qian-qian (1991-), female, doctor, major in 3D printing of aluminized explosive. e-mail: 18734914866@163.com

Corresponding author: NIE Fu-de(1969-), male, professor, major in design and preparation of energetic materials.e-mail: niefude@caep.cn

WANG Jun(1985-), male, assistant professor, major in design and characterization of composite materials. e-mail: wjun927@caep.cn

引用本文:贺倩倩,毛耀峰,王军,等. 制备梯度结构来提高HMX/Al复合材料的燃烧和压力输出性能[J]. 含能材料,2022,30(9):886-896.

HE Qian-qian, MAO Yao-feng, WANG Jun,et al. Preparation of Graded Structured HMX/Al to Enhance Combustion and Pressure Output Performance[J]. *Chinese Journal of Energetic Materials (Hanneng Cailiao)*,2022,30(9):886-896.

(ECP@Al) thermite could enhance pressure value and lower pressure boost rate. ZHAO Xu et al.[17] revealed that octahydro-1, 3, 5, 7-tetranitro-1, 3, 5, 7-tetrazocine/1, 3, 5-triamino-2, 4, 6-trinitrobenzene (HMX/TATB) co-particles exhibited higher pressure and detonation speed than that of HMX/TATB composite. WANG Jun et al.[18] designed and prepared the core-shell structured Al/polytetrafluoroethylene (Al/PTFE) to improve combustion reaction with enhanced pressure and energy output due to interfacial interaction. Compared with traditional microstructure design, bio-inspired structures from bamboo, bone, and nacre provide an effective approach to improve the properties of functional materials and devices. Relevant literatures[19-23] show that bio-inspired structures of advanced materials exhibit low density, high strength, and high energy absorption capacities. HUANG Jyun-kai and WANG You-yong et al.[24-25] reported that high strength and great toughness of bamboo stemmed from gradient composition distribution along the radial direction. Inspired by bamboo, component or density with gradient distribution has been applied in many fields, such as flexible electronics[26-27], hydrogels[28-29], and propellants[30]. The graded structure applied in flexible electronics not only enhanced their mechanical properties, but also enabled excellent foldability and electrochemical properties. In hydrogels, the bamboo-inspired structure could show excellent mechanical strength (the mechanical strength increased by 38%) and unique bending characteristics. The polymer composite with graded structure could possess significantly enhanced breakdown strength and energy density.

In our previous studies[31], based on the excellent properties of graded structure, the axially-graded structured HMX/Al with changed Al content was designed and prepared by additive manufacturing to enhance the pressure output. The results showed that the pressure output and pressurization rate could be divided into three stages, but the improvement of pressure output was not obvious due to limited structured characteristics and Al particle size distribution. In this work, to optimize combustion reaction and pressure output of HMX/Al cylinder, the radially-graded structured HMX/Al (RGS-HMX/Al) cylinder was designed with bamboo as inspiration. The three-layered RGS-HMX/Al cylinders with various content and particle size of Al was prepared by 3D direct writing technology. The combustion reaction and pressure output properties of RGS-HMX/Al cylinders were evaluated.

1 Experimental section

1.1 Materials

HMX powders (20 μm) were provided by Institute of Chemical Materials. Al powders (nAl: 160 nm, 5μAl: 5 μm, 10μAl: 10 μm) and ethyl acetate were purchased from Aladdin without further purification. Fluororubber was available from Zhonghao Chenguang Research Institute of Chemical Industry Co., Ltd.

1.2 Design and fabrication of RGS-HMX/Al cylinders

Bamboo shows high toughness and strength due to the gradient distribution of vascular bundles from the outer wall to the inner wall (Fig. 1a)[24-25]. Inspired by the microstructure of bamboo, RGS-HMX/Al cylinders were designed and prepared by 3D direct writing technology in this work (Fig. 1b).

For a typical preparation process, HMX, Al particles, and binder solution (ethyl acetate solution of fluororubber) were mixed by acoustic resonance technology to form HMX/Al ink. The rheological properties of HMX/Al composites were controlled by solvent evaporation, where HMX/Al ink obtained the characteristics of shear-thinning and storage modulus was greater than loss modulus. Then, the HMX/Al composites were put into syringe and printed to form the HMX/Al composite lines with the diameter of about 1.21 mm on the slide. On this basis, the HMX/Al composites were printed layer by layer to form the RGS-HMX/Al (Φ10×15 mm) cylinders with an outer layer, a middle layer, and an inner layer. Notably, the volume of each layer was the same, and the quality of cylinder was ~1.5 g. The component distribution of RGS-HMX/Al cylinders was shown in Table 1.

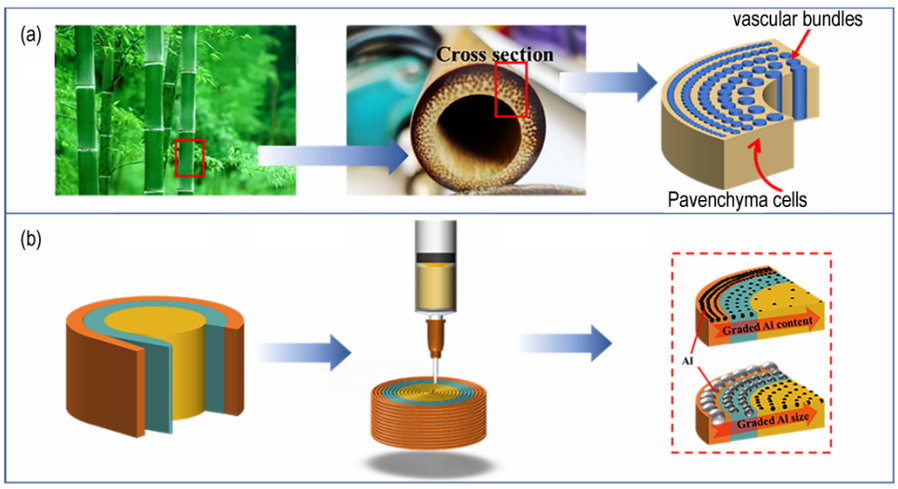

Fig.1 (a) Photograph of natural bamboo. (b) The fabrication process of RGS-HMX/Al cylinder with gradient content and size distribution of Al

Table 1 The component distribution of HMX/Al cylinders

sample type	cylinders	HMX/Al composites		
		inner layer	middle layer	outer layer
homogeneous HMX/Al	HnA-10	HMX/nAl-10%	HMX/nAl-10%	HMX/nAl-10%
	HnA-20	HMX/nAl-20%	HMX/nAl-20%	HMX/nAl-20%
	HnA-30	HMX/nAl-30%	HMX/nAl-30%	HMX/nAl-30%
	H5μA-30	HMX/5μAl-30%	HMX/5μAl-30%	HMX/5μAl-30%
	H10μA-30	HMX/10μAl-30%	HMX/10μAl-30%	HMX/10μAl-30%
	HA30-mix	HMX/nAl-30%, HMX/5μAl-30%, HMX/10μAl-30%		
RGS-HMX/nAl	HnA-1\2\3	HMX/nAl-10%	HMX/nAl-20%	HMX/nAl-30%
	HnA-3\2\1	HMX/nAl-30%	HMX/nAl-20%	HMX/nAl-10%
RGS-HMX/Al-30	HA30-n\10\5	HMX/nAl-30%	HMX/10μAl-30%	HMX/5μAl-30%
	HA30-5\10\n	HMX/5μAl-30%	HMX/10μAl-30%	HMX/nAl-30%
	HA30-5\n\10	HMX/5μAl-30%	HMX/nAl-30%	HMX/10μAl-30%
	HA30-10\n\5	HMX/10μAl-30%	HMX/nAl-30%	HMX/5μAl-30%
	HA30-n\5\10	HMX/nAl-30%	HMX/5μAl-30%	HMX/10μAl-30%
	HA30-10\5\n	HMX/10μAl-30%	HMX/5μAl-30%	HMX/nAl-30%

Note: 10% denotes that the quality fraction of Al is 10% in the HMX/Al composite.

1.3 Characterization

1.3.1 Morphology and structure analysis

Field emission scanning electron microscopy (FE-SEM, Ultra-55, Carl Zeiss, Germany) was used to characterize the morphologies of raw materials (Al, HMX) and RGS-HMX cylinders at 3 kV.

1.3.2 Thermal analysis

Thermogravimetry-differential scanning calorimetry (TG-DSC, PerkinElmer Diamond, America) was utilized to survey the heat-release characteristics of HMX/Al composites (~1.5 mg). The thermal temperature was conducted from 100 ℃ to 800 ℃ at a heating rate of 10 ℃·min^{-1} under N_2 flow rate of 40 mL·min^{-1}.

1.3.3 Combustion and pressure output measurement

The HMX/Al composite lines were ignited to study the combustion process by nickel-chrome wire (0.25 mm in diameter) with a direct current in the air atmosphere. The lines were ignited on the right, and the flame of combustion spread to the left. For the RGS-HMX/Al cylinders, the inner layer was ignited to obtain the combustion flame by CO_2 laser (laser power is 60 W, and spot diameter is 4 mm), and then the flame spread rapidly. The flame propa-

gation images of HMX/Al composite lines and RGS-HMX/Al cylinders were obtained by high-speed camera (Japan, UX50) with 500 fps. The combustion rate of HMX/Al composite lines was the average of calculated values based on three replicates for each sample.

To evaluate pressure output, the RGS-HMX/Al cylinders were ignited by nickel-chrome wire (about 5 cm in length) in a 330 mL explosion vessel. The signal of pressure change was collected by a pressure sensor with 20 MPa.

2 Results and Discussion

2.1 Morphology of RGS-HMX/Al

In order to better understand the microstructure of aluminized explosives for different formulations, the surface of cylinders is characterized by SEM. Fig. 2a shows the morphologies of Al and HMX powders. Evidently, Al particles present a regular spherical shape with mean particle diameter of 160 nm, 5 μm, and 10 μm, while HMX powders are rugged with mean size of 20 μm.

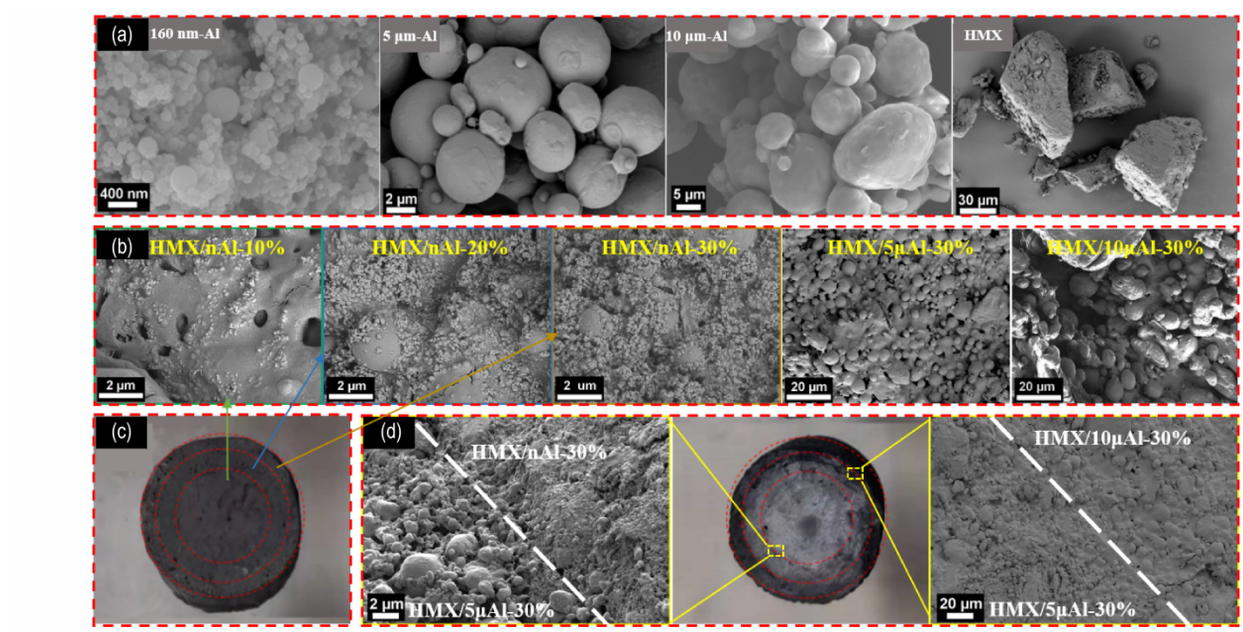

Fig.2 (a) SEM images of Al particles (160 nm, 5 μm, and 10 μm) and HMX in HMX/Al composite. (b) SEM images of HMX/Al composites. (c) The pictures of RGS-HMX/Al cylinder (HnA-1\2\3) with three layers from inner to outer. (d) SEM images of interface of different composites in RGS-HMX/Al cylinder (HA30-n\5\10)

Fig. 2b shows that the surface of HMX/Al composite is rugged with many bumps and micropores and becomes denser with increasing nAl content. The pores on the surface of HMX/Al composite are more obvious with the increase of Al particle size from 160 nm to 10 μm at the same content. In addition, the binder is evenly distributed between Al powders and HMX particles, which proves that HMX/Al composites have good uniformity and can well adapt to 3D printing. Fig. 2c shows the picture of bamboo-like RGS-HMX/Al cylinders (HnA-1\2\3) with different content distribution of Al manufactured by 3D direct writing technology. The adhesive effect of HMX/Al composites between adjacent formulations is better, and there is no obvious gap. Fig. 2d displays obvious interfaces between adjacent layers in HA30-n\5\10 cylinder (marked by white line in the figure), which indicates that the layers in RGS-HMX/Al cylinders contact with each other due to the action of binder.

2.2 Thermal analysis of HMX/Al composites

The HMX/Al composites exhibit a complex decomposition process, where two exothermic peaks and two distinct mass loss steps were observed as plotted in Fig. 3. As depicted in the DSC curves (Fig. 3a), there are two exothermic peaks. The first

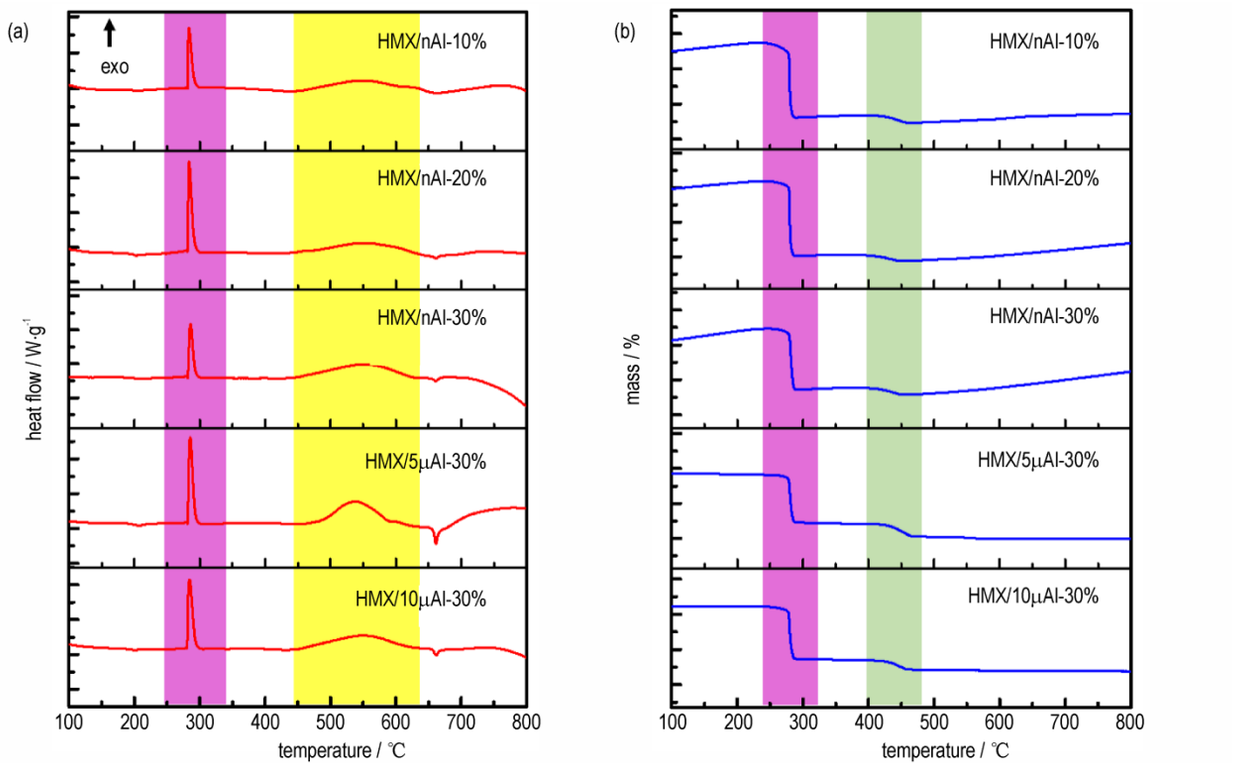

Fig.3 (a) DSC and (b) TG curves of HMX/Al composites

exothermic peak at 280 ℃ is the thermal decomposition of HMX, and the second exothermic peak is caused by the reaction between decomposition product and Al powders. The first reaction heat with the lowest value of 466.31 J·g^{-1} and the second reaction heat with the highest value of 1700.68 J·g^{-1} are calculated based on the DSC curves of HMX/nAl-30% composite. Table 2 shows the reaction temperature and heat value of HMX/Al composites. The reaction heat of HMX/nAl composites increases from 1767.61 J·g^{-1} to 2167.02 J·g^{-1} with increasing nAl content. More nAl powders participating in the reaction could release more heat. As for fixed Al content, HMX/nAl-30% composites have more heat release than that of HMX/5μAl-30% and HMX/10μAl-30% composites. It may be caused by the high specific surface area and activity of nAl powders.

Table 2 DSC parameters of HMX/Al composites with various Al

HMX/Al composites	T_1 / ℃	ΔH_1 / J·g^{-1}	T_2 / ℃	ΔH_2 / J·g^{-1}	ΔH / J·g^{-1}
HMX/nAl-10%	283.42	649.67	546.35	1117.94	1767.61
HMX/nAl-20%	285.87	561.43	550.16	1259.69	1821.12
HMX/nAl-30%	283.71	466.31	557.22	1700.68	2167.02
HMX/5μAl-30%	285.46	612.0	539.23	1341.41	1959.41
HMX/10μAl-30%	284.55	673.74	548.15	1282.20	1955.94

Note: T_1: The temperature of first exothermic peak, T_2: The temperature of second exothermic peak, ΔH_1: Heat value of first exothermic, ΔH_2: Heat value of second exothermic, ΔH: Total heat value of HMX/Al composite from 100 ℃ to 800 ℃.

The TG curves in Fig. 3b show the decomposition process of HMX/Al composites, which contain two obvious mass losses. The first mass loss is initiated by gas release, which is generated from the decomposition of HMX. The second step with an onset temperature of ~460 ℃ may be due to the thermal decomposition of fluororubber[32]. Then the reaction between exposed Al core and gaseous products (Al+HF→AlF_3+H_2) leads to the mass addition[33-34]. Notably, the mass increase of HMX/nAl-30% composites is larger than that of HMX/5μAl-30% and HMX/10μAl-30% composites. It may be due to the high specific surface area of nAl reacting with the oxidizer to form more AlF_3. The thermal reaction of HMX/Al provides a foundation to adjust combustion reaction and energy output for RGS-HMX/Al cylinders.

2.3 The combustion performance of RGS-HMX/Al cylinders

Combustion offers an important way for energy release of aluminized explosives, and the energy characteristics of aluminized explosives can also be understood through combustion flame. In order to better understand the combustion process of 3D printing gradient structure, the combustion performance of HMX/Al composite lines is firstly discussed. The effect of Al powder content on the combustion rate of HMX/Al composite lines has been discussed in our previous work[31]. With the increase of Al powder content, the combustion rate of HMX/Al composite line decreases. Here, the influence of Al particle size on the combustion performance of composite lines is mainly discussed with the fixed Al content of 30% with different particle sizes. The combustion process and combustion rate of HMX/Al composite lines are shown in Fig. 4.

From the perspective of combustion flame, the composite line of HMX/10μAl-30% displays the brightest flame and the largest flame area. By contrast, flame area and brightness decrease synchronously with decreasing Al particle size from 10 μm to 160 nm. The main reason is that Al particles with small particle size have fast heat conduction and combustion rate in the combustion process. Therefore, the combustion rate of HMX/Al composite lines decreases from 13 $mm \cdot s^{-1}$ to 11 $mm \cdot s^{-1}$ with increasing particle size of Al powders in the HMX/Al composite because of reduced heat conduction efficiency (Fig. 4d).

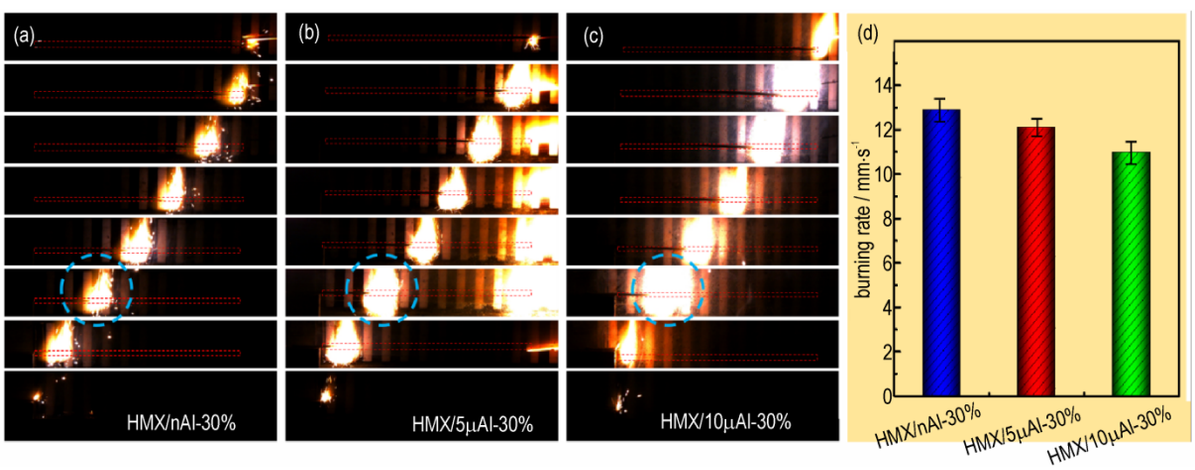

Fig.4 The combustion process of HMX/Al composite lines with different Al particle sizes of (a)160 nm,(b)5 μm, and (c)10 μm. (d) The burning rate of HMX/Al composite lines

The combustion process and flame propagation of RGS-HMX/Al cylinders are shown in Fig.5. Fig.5a shows the flame propagation process of HnA-1\2\3 cylinder with nAl content increasing from 10% (inner) to 30% (outer). Compared with HnA-20 cylinder (Fig.5b), the combustion flame of HnA-1\2\3 cylinder is more concentrated in the early stage showing a state of upward jet, and large flame area is obtained at a later stage. It is shown that the combustion reaction and flame propagation of inner layer is faster than that of outer layer, which may be resulted from low thermal decomposition temperature of HMX and the reaction between gaseous products and Al particles. The overall combustion efficiency and combustion time of HnA-1\2\3 cylinder are higher and less than that of homogeneous HMX/nAl-20% cylinder (HnA-20), respectively.

Fig. 5c shows the combustion phenomenon of HA30-10\5\n cylinder with a total Al content of 30% and Al sizes of 10 μm, 5 μm, and 160 nm from inner to outer layer. When HA30-10\5\n cylinder is ignited by the laser, a wide combustion flame area is obtained in a relatively short time range (about 1.9 s) and continuously propagates until the whole cylinder is completely burned[35]. Combined with the combustion performance of HMX/Al com-

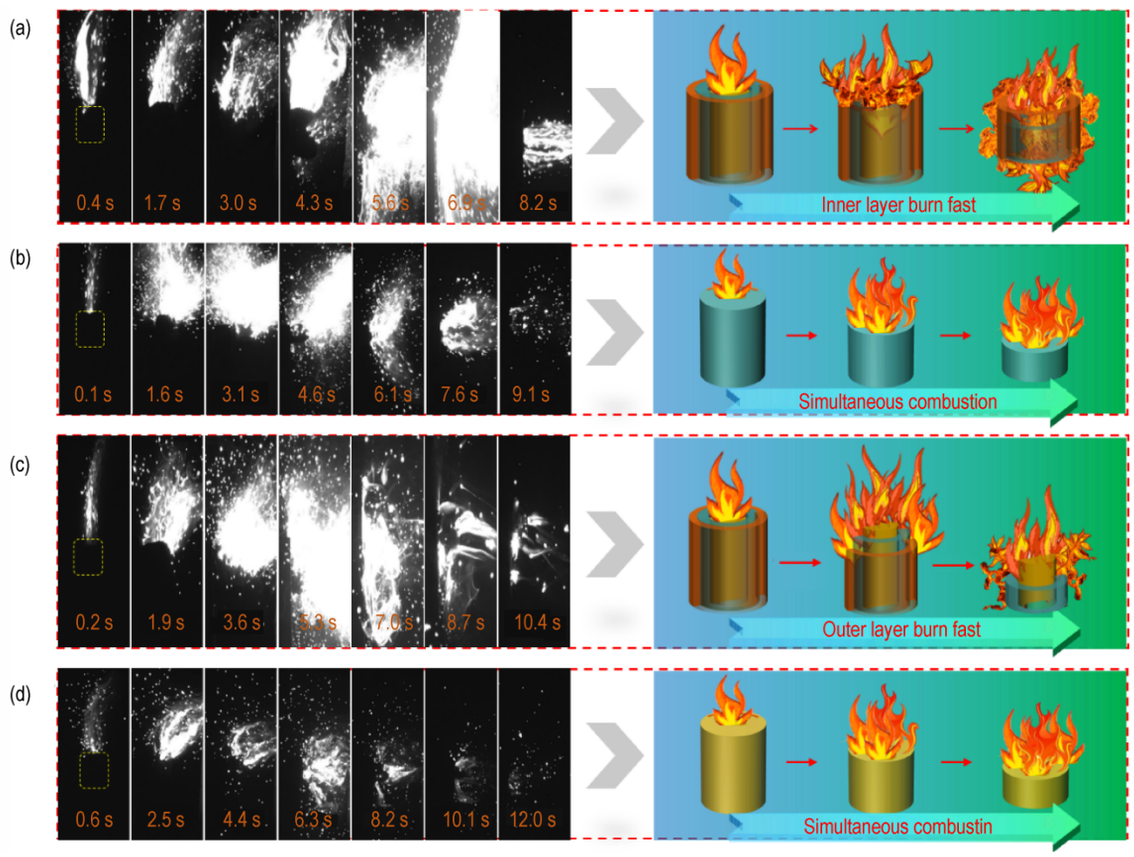

Fig.5 The combustion process and flame morphologies of RGS-HMX/Al cylinders, and the schematic diagram of combustion process. (a) The cylinder of HnA-1\2\3 (the nAl content are 10%, 20%, and 30% from inner to outer in the cylinder), (b) The cylinder of HnA-20, (c) The cylinder of HA30-10\5\n (the particle size of Al is 10 μm, 5 μm, and 160 nm from inner to outer layer in the cylinder), (d) The cylinder of HA30-mix with different Al particle size, and the Al particles randomly distribute in the cylinder

posite lines, it could be known that the bright flame is provided by the combustion of inner layer, and the subsequent continuous combustion depends more on HMX/5μAl-30% composite and HMX/nAl-30% composite with high burning rate in the middle and outer layer. Compared with the cylinder of HA30-mix (Fig. 5d), the RGS-HMX/Al cylinder (HA30-10\5\n) owns advantages in flame morphology and combustion efficiency.

2.4 Pressure output of RGS-HMX/Al cylinders

Compared with combustion, pressure impact is an efficient and wide-range way in the explosion of energetic materials, which is mainly based on explosion products and a large amount of gas damage to the target formation. The use of gradient structure provides an effective way to regulate the pressure output of aluminized explosives. In order to study pressure output process, HMX/Al cylinders are ignited on the top surface by nickel-chromium wire in a closed constant volume container to obtain pressure-time curve. RGS-HMX/nAl (HnA-1\2\3 and HnA-3\2\1) cylinders are used to illustrate pressure output performance. Fig. 6a shows the component distribution of HnA-1\2\3 cylinder. Fig. 6b~6c describe the curves of pressure-time for homogeneous and RGS-HMX/nAl cylinders in the combustion process. Based on the results, the peak pressure and pressurization rate increase with increasing Al content, which may be attributed to the secondary reaction of nAl and more energy release with high Al content.

The pressure output of RGS-HMX/nAl cylinders is significantly higher than that of homogeneous cylinders (HnA-10, HnA-20, and HnA-30). The re-

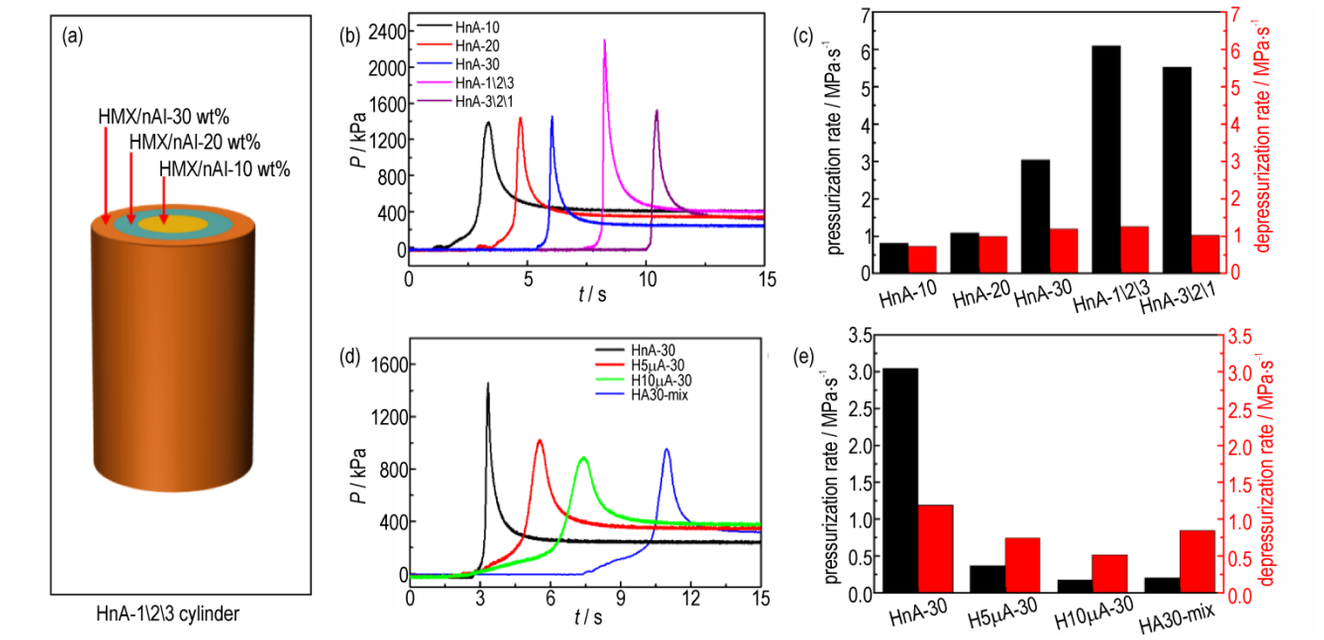

Fig.6 (a) The diagrammatic sketch of HnA-1\2\3. (b–c) The pressure-time curves, pressurization rate, and depressurization rate of homogeneous and RGS-HMX/nAl cylinders. The RGS-HMX/nAl cylinder with Al content from 10% to 30% shows significantly enhanced pressure output. (d–e) The pressure-time curves, pressurization rate, and depressurization rate of homogeneous HMX/Al with different sizes of Al particle in the combustion process

sults illustrate that the bio-inspired graded structure could enhance combustion reaction and pressure output, which may be due to the combustion propagation front of cylinder increased by different combustion rates between three layers, and the interfacial coupling between the layers driving the combustion of cylinder[36-37]. For RGS-HMX/nAl cylinder with the content of Al from 10% to 30% from inner to outer layer, the pressure peak is 2337.61 kPa and the pressurization rate is 6.09 MPa·s^{-1}. In comparison, RGS-HMX/nAl cylinder with Al content from 30% to 10% shows low values with the pressure peak of 1524.90 kPa and pressurization rate of 5.53 MPa·s^{-1}. The changed pressure peak of RGS-HMX/nAl cylinder with nAl distribution from inner to outer layer indicates that microstructure has a great influence on the combustion reaction and pressure output. The results can be applied to design and regulate combustion reaction and pressure output performance of HMX/Al.

To further investigate the effect of graded structure on pressure output performance, homogeneous HMX/Al cylinders with Al particle sizes of 160 nm, 5 μm, and 10 μm are prepared and tested, respectively. For comparison, we prepare the homogeneous HMX/Al-30% cylinder (HA30-mix) that contain three composite with different Al particle size is used. The pressure output and pressurization rate of cylinders are shown in Figs.6d and Fig.6e. The peak pressure and pressurization rate decrease from 1480.96 kPa and 3.04 MPa·s^{-1} to 729.95 kPa and 0.18 MPa·s^{-1} with Al particle size increasing from 160 nm to 10 μm, respectively. It may be caused by the long reaction time and low reaction kinetics of micron-Al powders[38-39].

Six typical RGS-HMX/Al-30 cylinders with different Al particle size distributions have been prepared and characterized to further illustrate the pressure output performance. Fig.7a shows the component distribution of HnA30-n\5\10 cylinder. The pressure-time curves of RGS-HMX/Al cylinders show a significant difference. For RGS-HMX/Al cylinders of HA30-n\10\5 and HA30-5\10\n, bimodal pressures are observed. When outer layer contains 5μ-Al, the first and second pressure peak are 397.48 kPa and 1155.65 kPa (Fig.7b), respectively. When outer layer

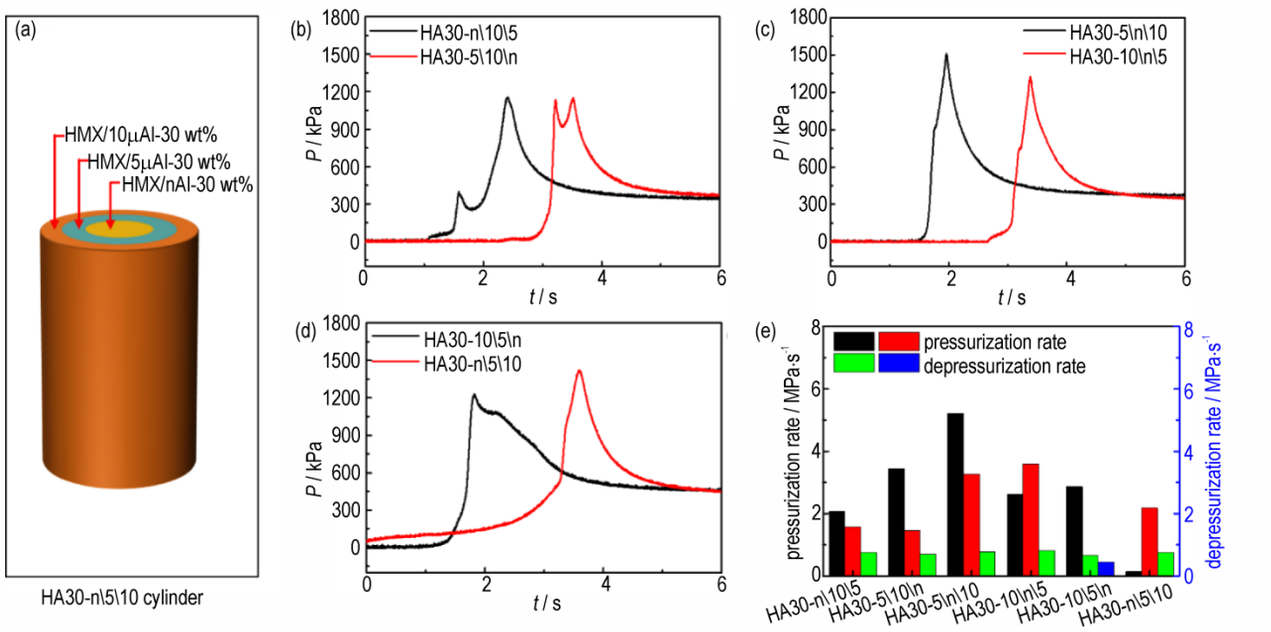

Fig.7 (a) The diagrammatic sketch of HA30-n\5\10 cylinder. (b–d) The pressure-time curves of RGS-HMX/Al-30 cylinders. (e) The pressurization rate and depressurization rate of RGS-HMX/Al-30 cylinders

contains nAl, the two pressure peaks are 1136.02 kPa and 1148.29 kPa, respectively. The bimodal pressures may be attributed to the reactivity of Al. Based on Refs.[40-41], the ignition and combustion of Al can be improved by reducing particle size. For RGS-HMX/Al cylinders of HA30-n\10\5 and HA30-5\10\n, the ignition and combustion reaction of Al in the inner and outer layer are faster than that of middle layer. Therefore, two peaks are obtained for RGS-HMX/Al cylinder.

For RGS-HMX/Al cylinders of HA30-5\n\10 and HA30-10\n\5, a variable pressurization rate is observed (Fig.7c). In the case of outer layer containing 10μ-Al, the pressurization rate reduces from 5.21 MPa·s^{-1} to 3.26 MPa·s^{-1}, and the pressure peak is 1512.65 kPa. When outer layer contains 5μ-Al, the pressurization rate increases from 2.63 MPa·s^{-1} to 3.59 MPa·s^{-1}, and the pressure peak is 1327.40 kPa. This phenomenon is caused by the fastest ignition and combustion reaction of nAl in the middle layer, which enable both inner and outer layers to expose in the air.

For RGS-HMX/Al cylinders of HA30-10\5\n, the depressurization rate decreases from 0.38 MPa·s^{-1} to 0.28 MPa·s^{-1} and the pressure peak is 1230.68 kPa (Fig 7d). Meanwhile, the pressurization rate from 0.14 MPa·s^{-1} to 2.17 MPa·s^{-1} and the peak pressure of 1422.46 kPa are observed for RGS-HMX/Al cylinders of HA30-n\5\10. It is also caused by gradually changing ignition and combustion reaction and the reactivity of Al powders. Above all, the pressure peak (1512.65 kPa) and the total pressurization rate (4.17 MPa·s^{-1}) of RGS-HMX/Al cylinder with the size of 5 μm, 160 nm, and 10 μm from inner to outer layer are the highest. The pressure peak and pressurization rate of homogeneous HMX/Al cylinder are 963.27 kPa and 0.21 MPa·s^{-1}(Fig.6), respectively, which is lower than that of RGS-HMX/Al cylinders.

3 Conclusion

The bio-inspired graded structure prepared by 3D direct writing technology could provide an effective approach to reinforce the combustion reaction and pressure output performances of HMX/Al for applications, and the experimental conclusions were as follows:

(1) The combustion reaction and flame propagation of HMX/Al composite cylinders could be improved by controlling the size and content distribution of Al from inner to outer layer.

(2) Significantly enhanced pressure values and gradient pressure output processes were obtained due to the graded structure of HMX/Al. The maximum pressure (2337.61 kPa) was obtained for the graded structure of HMX/nAl with content from 10% (inner layer) to 30% (outer layer).

(3) Bimodal pressures were observed for RGS-HMX/Al cylinders of HA30-n\10\5 and HA30-5\10\n. The graded structured HMX/Al with particle sizes of 5 μm, 160 nm, and 10 μm from inner to outer layer showed the highest peak pressure (1512.65 kPa) and pressurization rate (4.17 MPa·s^{-1}).

Reference:

[1] PEUKER J, KRIER H, GLUMAC N. Particle size and gas environment effects on blast and overpressure enhancement in aluminized explosives[J]. *Proceedings of the Combustion Institute*, 2013, 34(2): 2205-2212.

[2] BROUSSEAU P, DORSETT H E, CLIFF M D, et al. Detonation properties of explosives containing nanometric aluminum powder[C]//Proceedings of the 12th International Detonation Symposium. 2002. p. 11e21.

[3] JIANG Fan, WANG Xiao-feng, HUANG Ya-feng, et al. Effect of particle gradation of aluminum on the explosion field pressure and temperature of RDX-based explosives in vacuum and air atmosphere [J]. *Defence Technology*, 2019, 15(6): 844-852.

[4] TRZCINSKI W, MAIZ L. Thermobaric and enhanced blast explosives-properties and testing methods[J]. *Propellants, Explosives, Pyrotechnics*, 2015, 40(5): 632-644.

[5] TAPPAN B, MANNER V, LLOYD J, et al. Fast reactions of aluminum and explosive decomposition products in a post-detonation environment [C]//AIP Conference Proceedings. AIP (Chicago, USA, 26 June-1 July 2011). 2012, 1426: 271-274.

[6] DUAN Xiao-yu, GUO Xue-yong, JIAO Qing-jie, et al. Effects of Al/O on pressure properties of confined explosion from aluminized explosives [J]. *Defence Technology*, 2017, 13: 428-433.

[7] LIU Dan-yang, ZHAO Pin, CHAN S, et al. Effect of nano-sized aluminum on detonation characteristics and metal acceleration for RDX-based aluminum explosive[J]. *Defence Technology*, 2021, 17(2): 327-337.

[8] ZHOU Zheng-qing, NIE Jian-xin, OU Zhuo-Cheng, et al. Effects of the aluminum content on the shock wave pressure and the acceleration ability of RDX-based aluminized explosives[J]. *Journal of Applied Physics*, 2014, 116(14): 144906.

[9] XIANG Da-lin, RONG Ji-li, LI Jian. Effect of Al/O ratio on the detonation performance and underwater explosion of HMX-based aluminized explosives [J]. *Propellants, Explosives, Pyrotechnics*, 2014, 39 (1): 65-73.

[10] FENG Xue-song, FENG Xiao-jun, ZHAO Juan, et al. Effect of content and particle size of aluminum powder on the air blast property of HMX-based explosive [J]. *Explosive Materials*, 2018, 47(4): 10-15.

[11] ZHOU Zheng-qing, CHEN Jian-guo, YUAN Hong-yong, et al. Effects of aluminum particle size on the detonation pressure of TNT/Al[J]. *Propellants, Explosives, Pyrotechnics*, 2017, 42(12): 1401-1409.

[12] GOGULYA M, MAKHOV M, BRAZHNIKOV M, et al. Explosive characteristics of aluminized HMX-based nanocomposites[J]. *Combustion, Explosion, and Shock Waves*, 2008, 44(2): 198-212.

[13] HU Hong-wei, CHEN Lang, YAN Jia-jia, et al. Effect of aluminum powder on underwater explosion performance of CL-20 based explosives[J]. *Propellants, Explosives, Pyrotechnics*, 2019, 44(7): 837-843.

[14] TRZCINSKI W, CUDILO S, SZYMANCZYK L. Studies of detonation characteristics of aluminum enriched RDX compositions[J]. *Propellants, Explosives, Pyrotechnics*, 2007, 32(5): 392-400.

[15] MA Xiao-xia, ZHU Ying, CHENG Sheng-xian, et al. Energetic composites based on nano-Al and energetic coordination polymers (ECPs): The "father-son" effect of ECPs[J]. *Chemical Engineering Journal*, 2019, 392: 123719.

[16] MA Xiao-xia, CAO Ke, HUANG Xiao-na, et al. In situ synthesized MEMS compatible energetic arrays based on energetic coordination polymer and nano-Al with tunable properties[J]. *ACS Applied Materials & Interfaces*, 2020, 12(27): 30740-30749.

[17] ZHAO Xu, ZHANG Meng-hua, QIAN Wen, et al. Interfacial engineering endowing energetic co-particles with high density and reduced sensitivity [J]. *Chemical Engineering Journal*, 2020, 387: 126408.

[18] WANG Jun, QIAO Zhi-qiang, YANG Yun-tao, et al. Core-shell Al-polytetrafluoroethylene (PTFE) configurations to enhance reaction kinetics and energy performance for nanoenergetic materials[J]. *Chemistry A Europe Journal*, 2016, 22(1): 279-284.

[19] HA N, LU Guo-xing. A review of recent research on bio-inspired structures and materials for energy absorption applications[J]. *CompositeS Part B: Engineering*, 2020, 181: 107496.

[20] RUSCH F, WASTOWSKI A, LIRA T, et al. Description of the component properties of species of bamboo: A review[J]. *Biomass Conversion and Biorefinery*, 2021, 11: 28-30.

[21] HA N, Le V, GOO N. Investigation of punch resistance of the allomyrira dichtoloma beetle forewing[J]. *Journal of Bionic Engineering*, 2018, 15: 57-68.

[22] SYURIK J, SCHWAIGER R, SUDERAS P, et al. Bio-inspired micro-to-nanoporous polymers with tunable stiffness[J]. *Beilstein Journal of Nanotechnology*, 2017, 8: 906-914.

[23] XIN Zhi-bo, ZHANG Xiao-hui, DUAN Yu-gang, et al. Nacre-inspired design of CFRP composite for improved energy absorption properties[J]. *Composite Structures*, 2018, 184: 102-109.

[24] HUANG Jyun-kai, YOUNG Wen-bin. The mechanical, hygral, and interfacial strength of continuous bamboo fiber reinforced epoxy composites[J]. *Composite Part B: Engineering*, 2019, 166: 272-283.

[25] WANG You-yong, WANG Xiang-qian, LI Yuan-qing, et al. High-performance bamboo steel derived from natural bamboo[J]. *ACS Applied Materials & Interfaces*, 2021, 13(1): 1431-1440.

[26] SUN Yong-ming, SILLS R, HU Xian-luo, et al. A bamboo-inspired nanostructure design for flexible, foldable, and twistable energy storage devices[J]. *Nano Letters*, 2015, 15(6): 3899-3906.
[27] CAO Jie, ZHOU Ze-hang, SONG Quan-cheng, et al. Ultrarobust $Ti_3C_2T_x$ mxene-based soft actuators via bamboo-inspired mesoscale assembly of hybrid nanostructures[J]. *ACS Nano*, 2020, 14(6): 7055-7065.
[28] YIN Quan-yi, TU Shu-hua, CHEN min, et al. Bio-inspired design of reinforced gradient hydrogels with rapid water-triggered shape memory performance[J]. *ACS Applied Polymer Materials*, 2020, 2(7): 2858-2866.
[29] TAN Yun, XU Shi-mei, WU Long-lan, et al. A gradient laponite-crosslinked nanocomposite hydrogel with anisotropic stress and thermo-response[J]. *Applied Clay Science*, 2017, 148: 77-82.
[30] WANG Yi-fei, LI Yi, WANG Lin-xi, et al. Gradient-layered polymer nanocomposites with significantly improved insulation performance for dielectric energy storage[J]. *Energy Storage Materials*, 2020, 24: 626-634.
[31] HE Qian-qian, WANG Jun, MAO Yao-feng, et al. Fabrication of gradient structured HMX/Al and its combustion performance[J]. *Combustion and Flame*, 2021, 226: 222-228.
[32] MAO Yao-feng, HE Qian-qian, LI Zi-jian, et al. Rational design of gradient structured Fluorocarbon/Al composites towards tunable combustion performance[J]. *Combustion and Flame*, 2021, 230: 111436.
[33] KE Xiang. GUO Shuang-feng, ZHANG Gen-sheng, et al. Safe preparation, energetic performance and reaction mechanism of corrosion-resistant Al/PVDF nanocomposite films[J]. *Journal of Materials Chemistry A*, 2018, 36: C8TA05758C.
[34] CHEN Shu-wen, TANG De-yun. ZHANG Xue-xue, et al. Enhancing the combustion performance of metastable Al@AP/PVDF nanocomposites by doping with graphene oxide[J]. *Engineering*, 2020, 6(9): 1019-1027.
[35] XIAO Li-qun. FAN Xue-zhong, LI Ji-zhen, et al. Effect of Al content and particle size on the combustion of HMX-CMDB propellant[J]. *Combustion and Flame*, 2020, 214: 80-89.
[36] LI Xiang-yu, GURIERI P, ZHOU Wen-bo, et al. Direct deposit laminate nano-composite with enhanced propellant properties[J]. *ACS Applied Material & Interfaces*, 2015, 7(17): 9103-9109.
[37] WU Tao, LI Xiang-yu, HU Xiu-li, et al. Direct-deposition to create high particle loading propellants with controlled architecture: combustion and mechanical properties [C]//54th AIAA Aerospace Sciences Meeting, San Diego. 2016, 2: 0688.
[38] FEDOROV S, GUSEINOV S, STOROZHENKO P. Nano dispersed metal powders in high-energy condensed systems[J]. *Nano-technologies in Russia*, 2010, 5: 565-582.
[39] DELUCA L. Overview of Al-based nanoenergetic ingredients for solid rocket propulsion[J]. *Defence Technology*, 2018, 14(5): 357-365.
[40] DOKHAN A, PRICE E, SEITZMAN J, et al. The effects of bimodal aluminum with ultrafine aluminum on the burning rates of solid propellants[J]. *Proceedings of the Combustion Institute*, 2002, 29(2): 2939-2946.
[41] MURAVYEV N, FROLOV Y, PIVKINA A, et al. Influence of particle size and mixing technology on the combustion of HMX/Al composite[J]. *Propellants, Explosives, Pyrotechnics*, 2010, 35(2): 226-232.

制备梯度结构来提高HMX/Al复合材料的燃烧和压力输出性能

贺倩倩,毛耀峰,王　军,聂福德
(中国工程物理研究院化工材料研究所, 四川 绵阳 621999)

摘　要: 含铝炸药因其高能量密度和压力输出而被广泛应用。为了调控和提高含铝炸药的二次燃烧反应和压力输出,以竹子的微观结构为灵感设计了具有分级结构的HMX/Al径向梯度药柱,使用3D打印技术制备了不同铝含量和不同铝颗粒尺寸的HMX/Al径向梯度结构药柱,研究了Al含量和粒径分布对HMX/Al梯度结构燃烧性能和压力输出的影响。结果表明,当HMX/n-Al(160 nm)径向梯度结构按照从中心层向外层Al的质量分数分别为10%、20%和30%分布时,内层的燃烧反应和火焰传播速度比外层更快;其密闭空间内由于气体释放而获得的压力(2337.61 kPa)高于反向分布的梯度结构药柱。当HMX/Al径向梯度结构按照从中心层向外层Al粒径依次为10 μm-Al,5 μm-Al和n-Al分布时,梯度结构药柱的燃烧过程比较缓慢,可以看到单独铝颗粒的燃烧现象。当中间层为n-Al时,HMX/Al径向梯度结构具有最大的压力输出(1512.65 kPa),高于均相的HMX/Al药柱;当中间层为10 μm-Al时,获得了具有双重峰的压力输出。

关键词: 仿生结构;径向梯度结构;HMX/Al复合物;燃烧反应;压力输出
中图分类号: TJ55　　**文献标志码:** A　　**DOI:** 10.11943/CJEM2022067
基金项目: 国家自然科学基金资助(11872341和22075261)

(责编:王馨逸)